Supporting Information

Stewart-Jones et al. 10.1073/pnas.0901425106

SI Materials and Methods

MHC-Peptide Monomers. The HLA-A*0201 heavy chain with a C-terminal biotinylation tag, ß2m, and the respective HLA-A*0201-restricted peptides were refolded by dilution as previously described (1, 2). For crystallography, HLA-A*0201 heavy chain without the biotinylation tag was used for refolding, and purified as described (3).

Antibody Crystallization and Data Collection. The 3M4E5-A2-NYESO-1 complex crystallized in 14% PEG 8000 50 mM Mes (pH 6.5) with crystal dimensions of ≈110 μm by 60 × 30 μm. The 3M4F4-A2-NYESO-1 complex crystallized in 12% PEG 8000 50 mM Mes (pH 6.9) with crystal dimensions of ≈50 × 35 × 10 μm. The 3M4E5 Fab crystallized in 14% PEG 8000 50 mM Mes (pH 6.5) with crystal dimensions of about 50 × 40 × 20 μm. Crystals were harvested and briefly soaked sequentially in reservoir solutions containing 10% and 20% glycerol, then flash cooled and maintained at 100 K in a cryostream (Oxford Cryosystems). Datasets were collected at station ID14eh2 of the ESRF (European Synchrotron Radiation Facility) using an ADSC-Q4 (Area Detector Systems Corporation) charged-coupled device (CCD) detector. Datasets were autoindexed and integrated with the program DENZO followed by scaling with the program SCALEPACK (4). The results are summarized in supporting information (SI) Table S2.

Structure Determination and Refinement. All structures were determined by molecular replacement in PHASER (5) using the peptide-MHC class I molecule from the HLA-A*0201-NYESO-1–1G4 TCR complex (PDB ID code 2BNQ) and the Fab fragment from PDB entry 1RZF as search coordinates. Initial rigid-body refinement of individual domains (α1α2, α3, β2M, peptide, VH, VL, CH, and CL) followed by restrained TLS refinement was performed in REFMAC5 (6). Manual rebuilding was carried out in COOT (7) and water picking in the final stages of refinement was performed with ARPw/ARP (8). All regions of the Fabs and HLA-A*0201-NY-ESO-1 were included in the final models except for residues 154–159 from the light chain (chain L) of the 3M4E5-HLA-A*0201-NYESO-1 complex where no electron density was detectable. Crystallographic statistics for the final models are given in Table S2. Figures were generated in CCP4MG (9).

Phage Display Selection. Phage Fab particles were produced and incubated with HLA-A*0201/NY-ESO-$1_{157–165}$ complex in the presence of Fab 3M4E5 protein (100 μg/mL) following the selection procedure as previously described (2). Bound phages were eluted with 100 mM triethylamin and neutralized with Tris-HCl (pH 7.2). Phages were used to infect *E. coli* strain *TG1* (30 min, 37 °C), and bacteria were grown on agar (ON, 30 °C). Analysis of genetic distance for individual clones was performed using the cluster analysis program ClustalW (European Bioinformatics Institute, http://www.ebi.ac.uk/clustalw/).

Antibody Binding Assays. The specificity of individual phage clones and soluble Fab antibodies was assessed by ELISA at room temperature with indirectly coated MHC-class I antigen peptide complexes (2). Correct folding of complexes was confirmed by monoclonal antibodies W6/32 and BB7.2 (Jackson). Recombinant soluble Fab antibodies were purified from *E. coli* periplasmic fraction as described (2), and bound Fab molecules were detected by murine anti-myc antibody 9E10 (0.3 μg/mL; Roche). M13 antibody (0.3 μg/mL) (Amersham Pharmacia Biotech) was used for the detection of phage particles. A horseradish peroxidase-conjugated antibody (anti-mouse IgG, 1:2000; Dako) was used as secondary reagent. Tetramethylbenzidine was used as substrate (Sigma).

Antibody Binding Affinity by Surface Plasmon Resonance (SPR). SPR studies were performed using a Biacore™ 3000 (Biacore AB) as previously described (2, 10). HLA-A*0201-SLLMWITQC and HLA-A*0201-SLLMWITQV were enzymatically biotinylated by BirA enzyme on the C-terminal biotinylation site and immobilized to CM5 sensor chips via covalently coupled streptavidin. Kinetic constants were derived using the curve-fitting facility of the BIAevaluation program (version 3.0; Biacore AB) and rate equations derived from the simple 1:1 Langmuir binding model (A+B↔ AB). Duplicates of each measurement were performed and averaged.

Flow Cytometry. Stable-transfected HLA-A0201-positive T2 cell lines expressing various HLA-A0201-restricted NY-ESO-1 peptides (so-called minigenes; 1a = NY-ESO-1 peptide 157–167, 1b = 157–165, and 1c = 155–163) or peptide-pulsed (2 h, 37 °C) T2 cells (3×10^4) were used to verify binding specificity of selected phages and Fabs, respectively (2). Cells were incubated with different Fabs at indicated concentrations in 100 μL PBS-BSA (30 min, 4 °C), washed in PBS-BSA, and binding visualized by a 2-step procedure using antibody 9E10 (5 μg/mL; 30 min, 4 °C) and a PE-conjugated/anti-mouse IgG (dilution 1:10, Dianova; 30 min, 4 °C). Staining with w6/32 and BB7.2 antibody confirmed presence of HLA molecules.

An inhibition assay was set up using a suboptimal concentration of PE-conjugated 3M4E5-b tetramer. 3M4E5-Fab tetramers were assembled by incubating 60 μg biotinylated 3M4E5-Fab monomers with 80 μg of streptavidin-conjugated R-PE (Invitrogen; 45 min, 37 °C or ON, 4 °C) at an optimal stoichometric ratio of 1:4. The suboptimal 3M4E5 tetramer concentration was determined on T2–1b minigene cells or T2 cells pulsed with the respective NY-ESO-1 peptide (SLLMWITQV) (pulsing conditions: 2 h 37 °C, peptide concentration: 10^{-5}–10^{-10}M). Cells were then incubated with 3M4E5 tetramer (1 h, 4 °C), washed twice with PBS-Tween 0.05%, and varying concentrations (0.0005–50 μg/mL) of candidate Fabs (45 min, 4 °C) added. All data were acquired by flow cytometry (FACScan, Becton Dickinson) and analyzed with WinMDI program (J. Trotter, http://facs.scripps.edu/).

T-Cell Inhibition. Assays were performed in a modified ELISPOT assay in triplicates on nitrocellulose-lined 96-well plates (MAHA S45 by Millipore). Wells were precoated overnight with an anti-IFN-γ capture antibody as recommended (Mabtech AB) and blocked (1 h, 37 °C) with RPMI containing 10% human serum. The $CD8^+$ HLA-A2/NY-ESO-$1_{157–165}$-specific T cell clone was cultured as previously described (11). Target T2 cells were pulsed with 0.1 μg/mL of NY-ESO-$1_{157–165}$ peptide (1 h, 37 °C), stringently washed, and incubated (1 h, 37 °C) with different concentrations (30, 3, 0.3, 0.003, 0.0003, 0.00003, 0 μg/mL) of HLA-A0201*/NY-ESO-$1_{157–165}$ complex-specific or -irrelevant Fab antibodies. $CD8^+$ T cells were cocultured with target cells for 16 h at 37 °C (E:T of 1:1, i.e., 8000:8000 cells per well). Plates were evaluated using an automated ELISPOT reader (Bioreader 3000, BioSys).

Generation and Functional Analysis of Recombinant T-Cell Receptors. Candidate Fab antibodies were converted into scFv fragments, flanked by NcoI and BamHI restriction sites, and cloned into the pBullet vector (12) containing human CD3 zeta and CD28 signaling domains (13). An anti-CEA scFv construct served as control. Retroviral transduction of $CD3^+$ T cells with recombinant receptors was previously described in detail (13). Receptor expression was monitored by flow cytometry using PE-labeled HLA-A*0201/NY-ESO-$1_{157–165}$ tetramers. T cells grafted with the recombinant immunoreceptors were cocultivated in round-bottom 96-well microtiter plates at different numbers (ranging from 0.075–10 $\times$ 10^3 receptor grafted T cells per well) with HLA-A2/NY-ESO-$1_{157–165}$-positive and -negative T2 cells (5 $\times$ 10^3 cells per well). After 24 h, culture supernatants were analyzed for IFN-γ release using a sandwich ELISA [(coat mAb NIB42 (1 μg/mL; Pierce) detection by biotinylated mAb 4S.B3 (0.5 μg/mL; BD Bioscience)]. The reaction was visualized by peroxidase streptavidin (1:10,000) and ABTS (both by Roche Diagnostics).

Specific cytotoxicity of receptor-grafted T cells against target cells was analyzed using a colorimetric tetrazolium salt-based assay indicating cell viability (EZ4U; Biomedica) as described (13, 14). Briefly, $CD3^+$ T cells expressing NY-ESO-1-specific immunoreceptors were cocultivated as described. After 24 h, XTT (1 mg/mL) (Cell Proliferation Kit II, Roche Diagnostics) was added to the cells and incubated for 30–90 min at 37 °C. Reduction of XTT to formazan by viable tumor cells was colorimetrically monitored (adsorbance wavelength 450 nm, reference wavelength 650 nm). Maximal reduction of XTT was determined as the mean of 6 wells containing target cells only, and the background as the mean of 6 wells containing RPMI medium 1640, 10% (vol/vol) FCS. The nonspecific formation of formazan due to the presence of effector cells was determined from triplicate wells containing effector cells in the same number as in the corresponding experimental wells. The viability of tumor cells was calculated as follows:

$$\text{viability}\,[\%] = \frac{\text{OD}_{(\text{exp. wells} - \text{corresponding number of effector cells})}}{\text{OD}_{(\text{tumor cells without effectors} - \text{medium})}} \times 100$$

1. Altman JD, et al. (1996) Phenotypic analysis of antigen-specific T lymphocytes. *Science* 274(5284):94–96.
2. Held G, et al. (2004) Dissecting cytotoxic T cell responses towards the NY-ESO-1 protein by peptide/MHC-specific antibody fragments. *Eur J Immunol* 34(10):2919–2929.
3. Madden DR, Garboczi DN, Wiley DC (1993) The antigenic identity of peptide-MHC complexes: A comparison of the conformations of five viral peptides presented by HLA-A2. *Cell* 75(4):693–708.
4. Otwinowski ZM, Minor W (1997) Processing of X-ray diffraction data collected in oscillation mode. *Methods Enzymol* 276:307–326.
5. McCoy AJ, Grosse-Kunstleve RW, Storoni LC, Read RJ (2005) Likelihood-enhanced fast translation functions. *Acta Crystallogr D Biol Crystallogr* 61(Pt 4):458–464.
6. Murshudov GN, Vagin AA, Dodson EJ (1997) Refinement of macromolecular structures by the maximum-likelihood method. *Acta Crystallogr D Biol Crystallogr* 53(Pt 3):240–255.
7. Emsley P, Cowtan K (2004) Coot: Model-building tools for molecular graphics. *Acta Crystallogr D Biol Crystallogr* 60(Pt 12 Pt 1):2126–2132.
8. Morris RJ, Perrakis A, Lamzin VS (2003) ARP/wARP and automatic interpretation of protein electron density maps. *Methods Enzymol* 374:229–244.
9. Potterton L, et al. (2004) Developments in the CCP4 molecular-graphics project. *Acta Crystallogr D Biol Crystallogr* 60(Pt 12 Pt 1):2288–2294.
10. Willcox BE, et al. (1999) TCR binding to peptide-MHC stabilizes a flexible recognition interface. *Immunity* 10(3):357–365.
11. Zippelius A, et al. (2004) Effector function of human tumor-specific CD8 T cells in melanoma lesions: A state of local functional tolerance. *Cancer Res* 64(8):2865–2873.
12. Weijtens ME, Willemsen RA, van Krimpen BA, Bolhuis RL (1998) Chimeric scFv/gamma receptor-mediated T-cell lysis of tumor cells is coregulated by adhesion and accessory molecules. *Int J Cancer* 77(2):181–187.
13. Hombach A, et al. (2001) Tumor-specific T cell activation by recombinant immunoreceptors: CD3 zeta signaling and CD28 costimulation are simultaneously required for efficient IL-2 secretion and can be integrated into one combined CD28/CD3 zeta signaling receptor molecule. *J Immunol* 167(11):6123–6131.
14. Jost LM, Kirkwood JM, Whiteside TL (1992) Improved short- and long-term XTT-based colorimetric cellular cytotoxicity assay for melanoma and other tumor cells. *J Immunol Methods* 147(2):153–165.

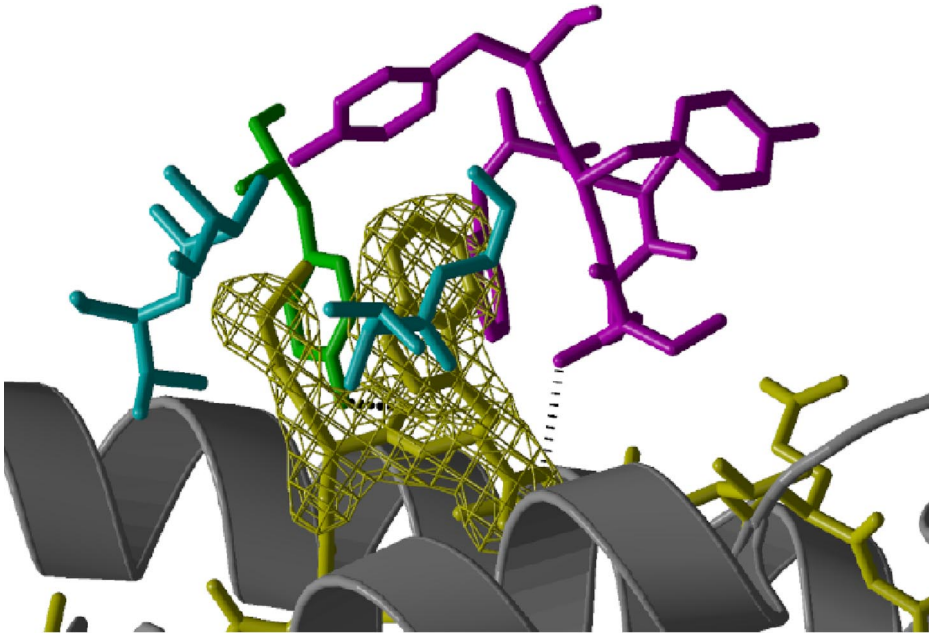

Fig. S1. Simulated annealing omit electron density map showing the peptide MW residues bound by the 3M4F5 Fab in yellow chicken wire. Fab residues are colored according to the CDR color as in Fig. 1*D*. Hydrogen bonds between the Fab and the MW residues are shown in black. The map is contoured at 3σ.

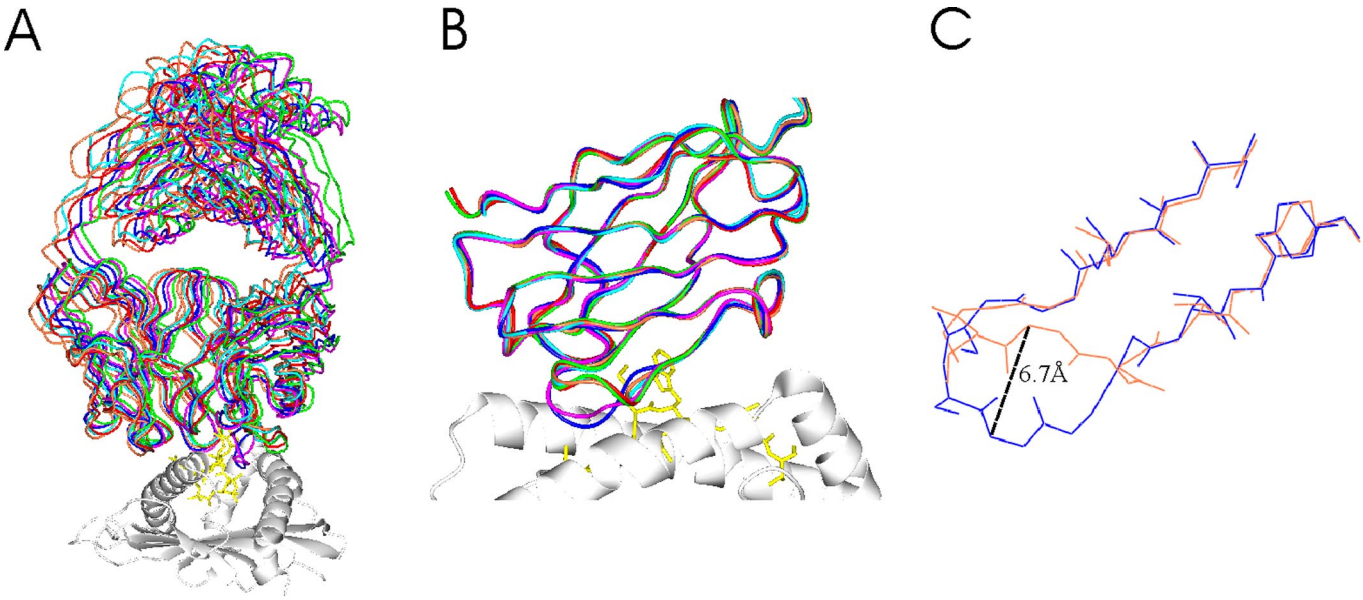

Fig. S2. (*A*) Superposition, based on the MHC α1/α2 helices, of the two 3M4E5 and four 3M4F4 Fab complexes found in the crystallographic asymmetric unit, illustrating the variable positioning of the Fabs in the different crystal contexts. Colors are for 3M4E5 chains H/L, green; K/M, red; and for 3M4F4 H/L, blue; G/I, magenta; N/O, cyan, and S/T, coral (chain labels correspond to those for the deposited PDB files). MHC is colored gray and the NYESO-$1_{157–165}$ peptide yellow. (*B*) Superposition, based on the VH domains, of all 6 bound Fab structures (3M4E5 chains H and K, 3M4F4 chains H, I, O, and T), illustrating the ''down'' conformation of the CDR2 VH loop found in chains H and I of the 3M4F4 Fab, where in all of the other Fab structures, the CDR2 adopts the ''up'' conformation. (*C*) Superposition of the VH domains from representative 3M4F4 structures for the 2 CDR2 VH conformations, chains H (blue) and T (coral), illustrating the 7 Å main-chain change and side chain reorientations.

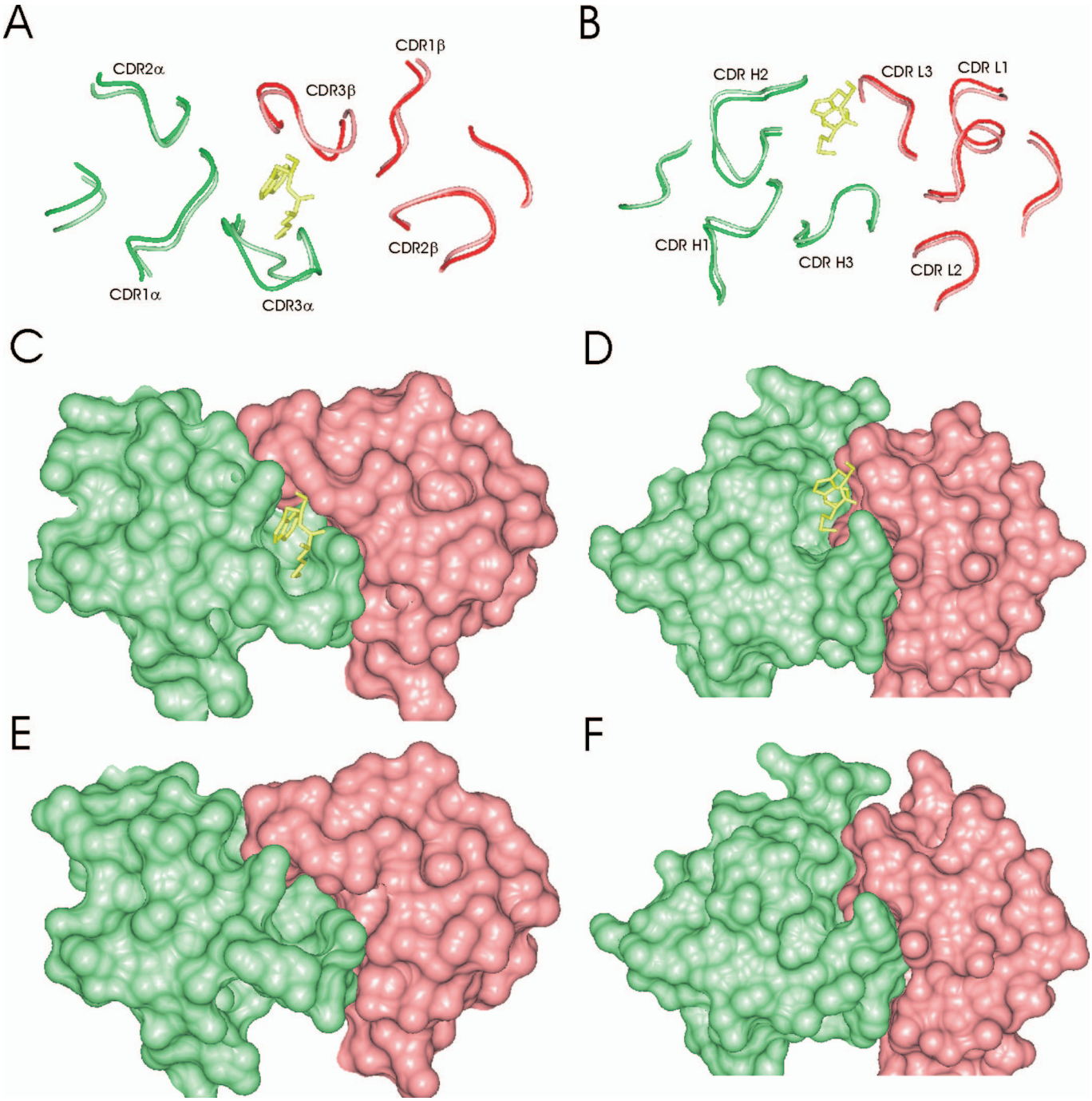

Fig. S3. Conformational changes on binding for (*A*) the 1G4 TCR (alpha chain is green and beta chain is red, unliganded structures are in light colors) and (*B*) the 3M4F5 Fab (heavy chain is green and light chain is red; unliganded structures are in light colors) where minor conformational adjustments are apparent for the 1G4 TCR compared with almost no significant main chain conformational adjustment of the 3M4E5 Fab CDR loops. The peptide MW residues are illustrated in yellow. Molecular surfaces (colored as above) for the liganded (*C*) and unliganded (*E*) 1G4 TCR, and the liganded (*D*) and unliganded (*F*) 3M4E5. For both, 1G4 and 3M4E5, a cavity is preformed in the unliganded structures that can accommodate the peptide MW side chains (*E* and *F*).

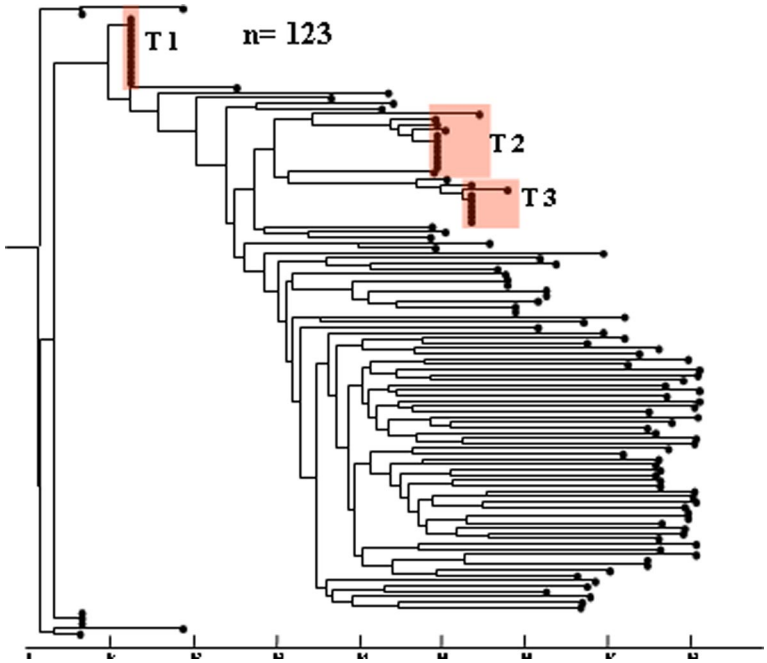

Fig. S4. Classification of 3M4E5 mutants by phylogenetic tree analysis. Amino acid sequences of mutated regions were subjected to cluster analysis using ClustalW software for 123 mutant clones. The following conditions were used: matrix, BLOSUM; gap opening penalty, 10.0; gap extension penalty, 0.05. Results are displayed as a phylogenetic tree, which indicates the genetic distance to the parental 3M4E5 sequence. The 3 types of mutants that were repeatedly identified are indicated in red.

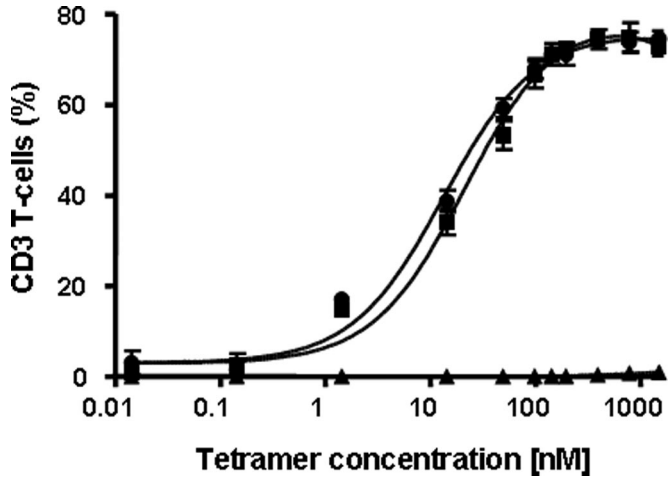

Fig. S5. Tetramer staining of transduced T cells. Binding specificity of T1(circles), WT (squares), and control (triangles) sc-TCRs on transduced $CD3^+$ T cells were analyzed by incubation with indicated amounts of PE-conjugated HLA-A*0201/NY-ESO-$1_{157–165}$ tetramers using flow cytometry. Assay was done in triplicates and SD is depicted.

Table S1. Crystallographic data collection and refinement statistics

	3M4E5-A2-NYESO-1, 1.9 Å	3M4F4-A2-NYESO-1, 2.9 Å	3M4E5, 2.3 Å
Data collection	$P2_1$	$P2_1$	P43
Space group			
Unit cell			
dimensions, Å (a, b, c)	71.6, 111.8, 124.7	70.8, 105.6, 256.5	117.1, 117.1, 78.9
Angles, degrees (α, β, γ)	90, 93.5, 90	90, 92.3, 90	90, 90, 90
Molecules/complexes in AU	2	4	2
Source	ESRF ID14-eh2	ESRF ID14-eh2	ESRF ID14-eh2
Resolution, Å			
(highest-resolution shell)	30–1.9 (1.97–1.90)[a]	30–2.9 (2.70–2.9)[a]	30–2.3 (2.45–2.3)[a]
Measured reflections	977,096	539,019	428,360
Unique reflections	153,950	84,609	24,603
Completeness (%)	100 (99.9)[a]	97.8 (88.5)[a]	99.0 (92.1)[a]
I/σ (I)	23.0 (2.6)[a]	14.2 (2.6)[a]	40.9 (4.4)[a]
R_{merge} (%)[b]	7.2 (72.7)[a]	11.8 (52.3)[a]	6.5 (63.1)[a]
Refinement Statistics			
Resolution range (Å)	30–1.9 (1.97–1.90)[a]	30–2.9 (3.0–2.9)[a]	30–2.3 (2.45–2.3)[a]
R_{cryst}[b]	20.2	20.2	22.2
R_{free}[d]	25.2	28.3	30.2
Number of non-H protein atoms	12,715	25,434	6,412
Number of water molecules	1,606	0	379
Rms deviation from ideality			
Bond lengths, Å	0.014	0.017	0.021
Bond angles, degrees	1.61	1.82	1.946
Ramachandran plot, % (favored, allowed, generous, disallowed)	(84.7, 13.6, 1.1, 0.6)	(86.0, 12.1, 1.2, 0.7)	(85.1, 13.0, 1.3, 0.7)

[a]Numbers in parentheses correspond to the outermost shell of data.
[b]$R_{merge} = \Sigma_{hkl}|I - <I>|/\Sigma_{hkl}I$, where I is the intensity of unique reflection hkl and $<I>$ is the average over symmetry-related observations of unique reflection hkl.
[c]$R_{cryst} = \Sigma||F_{obs}| - |F_{calc}||/\Sigma|F_{obs}|$, where F_{obs} and F_{calc} are the observed and calculated structure factors, respectively.
[d]R_{free} is calculated as for R_{cryst} but using 5.0% of reflections sequestered before refinement.

Table S2. Interactions between 1G4 TCR Vα and Vβ domains and the HLA-A*0201- NY-ESO-$1_{157–165}$ (<4.0 Å)

Direct interactions (<4.0 Å)

Element	1G4 TCR contact residue	HLA-A2 contact residue
Vα CDR1	Y31	Q155
Vα CDR2	Q51	A150, H151, Q155
Vα CDR2	S52	Q155
Vα CDR2	S53	Q155, E154
Vα CDR2	S54	H151, E154
Vα CDR3	G97	R65
Vα CDR3	G98	R65, K66
Vα CDR3	S99	R65
Vα CDR3	Y100	K66
Vβ CDR1	E29	Q72, T73
Vβ CDR2	Y47	R65
Vβ CDR2	V49	R65, Q72
Vβ CDR2	G50	Q72
Vβ CDR2	A51	Q72
Vβ CDR2	I53	K68
Vβ CDR2	D55	R65
Vβ CDR2	T70	Q72
Vβ CDR3	V95	T73
Vβ CDR3	N97	A150
		Peptide contact residue
Vα CDR1	Y31	W5
Vα CDR3	R93	W5
Vα CDR3	P94	M4, W5
Vα CDR3	T95	M4, W5
Vα CDR3	S96	M4
Vα CDR3	G97	M4
Vα CDR3	G98	M4
Vα CDR3	Y100	M4
Vβ CDR1	N27	Q8
Vβ CDR1	E29	Q8
Vβ CDR3	Y94	Q8
Vβ CDR3	V95	M4, W5, I6
Vβ CDR3	G96	W5, I6, T7
Vβ CDR3	N97	T7

Table S3. Interactions between Fab 3M4E5 VL and VH domains and the HLA-A*0201- NY-ESO-$1_{157–165}$ (<4.0 Å)

Direct interactions (<4.0 Å)

Element	3M4E5 contact residue	HLA-A2 contact residue
VH CDR2	V52	T163
VH CDR2	S54	E166, T167
VH CDR2	G55	T163
VH CDR2	G56	A158, T163
VH CDR2	S57	T163, Y159
VH CDR2	T58	A158, Q155
VH CDR2	A59	Q155
VH CDR2	K65	A150, H152
VH CDR3	L101	R65
VH CDR3	P102	R65
VH CDR3	Y103	R65, K66, A69
VH CDR3	Y104	R65
VL CDR1	G31	Q72
VL CDR1	Y32	Q72, A69, T73
VL CDR1	Y34	R65
VL CDR2	D52	R65
VL CDR3	S96	Q155
		Peptide contact residue
VH CDR2	S57	W5
VH CDR2	T58	W5
VH CDR2	A59	W5
VH CDR3	P102	M4
VH CDR3	Y103	M4
VL CDR1	S26	Q8
VL CDR1	R27	Q8
VL CDR1	Y32	Q8
VL CDR3	F93	M4, W5
VL CDR3	G95	W5, I6
VL CDR3	S96	W5, T7
VL CDR3	Y97	W5
VL CDR3	Y98	M4, W5

Table S4. Listing of the 3 most frequent sequence patterns selected from the second-generation phage display library

	Light chain						Heavy chain							
Amino acid position	26	27	32	95	96	97	33	35	50	52	57	59	99	Frequency of clones
3M4E5	S	R	Y	G	S	Y	Q	S	G	V	S	A	E	
Fab T1	**E**	R	Y	G	**G**	Y	Q	S	G	V	S	A	E	$n = 15$
Fab T2	**E**	R	Y	G	**G**	Y	**E**	**H**	**V**	**L**	**E**	**N**	**M**	$n = 11$
Fab T3	**E**	R	Y	G	**G**	Y	**Y**	**D**	**T**	**A**	**E**	A	**S**	$n = 11$

Only residues that were randomized as selection strategy are depicted. Amino acid positions are given as Kabat numbers (http://www.hgmp.mrc.ac.uk).